Electronic Supplementary Materials

Engineering the Coordination Geometry of Metal-organic Complex Electrocatalysts for Highly Enhanced Oxygen Evolution Reaction

Dafeng Yan[+], Chung-Li Dong[+], Yu-Cheng Huang[+], Yuqin Zou,* Chao Xie, Yanyong Wang, Yiqiong Zhang, Dongdong Liu, Shaohua Shen, and Shuangyin Wang*

Experiment section

Phy-Co^{2+} was prepared through a facile one-step coprecipitation method according to the published work. In a typical process, 0.5 mmol sodium phytate was dissolved in 5 mL of distilled water on the condition of ultrasound (solution A). Then the prepared 10 mL of 3 mmol mixture solution containing cobalt (II) nitrate hexahydrate was added into solution A slowly with stirring. And pink sediment was formed immediately. The sediment was washed with water and ethanol for three times and drying at 60 °C for 10 h. The initial samples were put in the plasma reactor. The plasma treated samples were synthesized by Ar DBD plasma at the condition of 80 V and 2.5 A for different times. And the Phy-Co^{2+}/Fe^{3+} was just prepared at the same condition as Phy-Co^{2+}, except that change the pure cobalt nitrate solution to cobalt nitrate and iron (III) nitrate solution with a certain mole ratio.

Materials characterization

The morphology was investigated by scanning electron microscope (SEM, Hitachi, S-4800) and transmission electron microscopy (TEM, Tecnai g2 F20, and aberration-corrected STEM). X-ray powder diffraction (XRD) was carried out on a Siemens

D500 diffractometer with a Cu Kα source (1.54056Å). The X-ray photoelectron spectroscopy (XPS) analysis was performed on an ESCALAB 250Xi X-ray photoelectron spectrometer using Mg as the excitation source. EPR experiments were performed on a Bruker EMX X-band spectrometer and microwave frequency = 9.40 GHz at room temperature. A 300W-Xe lamp with a 420 nm cutoff filter was used for light irradiation EPR measurement. The synchrotron X-ray spectroscopic measurements at Co K-edge were performed at the National Synchrotron Radiation Research Center (NSRRC), Taiwan.

Electrochemical measurements

Electrochemical measurements of the samples for HER were carried out using an electrochemical workstation (CHI 760E, CHInstrument, USA) with a typical three-electrode system at the room temperature through both CV and LSV. For electrochemical measures of OER, the catalyst dropped on a glassy carbon electrode was used as the working electrode, saturate calomel electrode (SCE) was used as the reference electrode in 1 M KOH electrolyte, and platinum gauze was used as the counter electrode. The scan rate for LSV was kept at 5 mV s^{-1} to minimize the capacitive current. In addition, the LSV polarization curves for OER were measured in saturating the solution with O_2. The scan rate for LSV was kept at 5 mV s^{-1} respectively. All the polarization curves in this work were corrected by eliminating iR drop with respect to the ohmic resistance of the solution. Calibration of SCE reference electrodes was done by measuring the reversible hydrogen electrode (RHE) potential using a Pt electrode under a H_2 atmosphere.

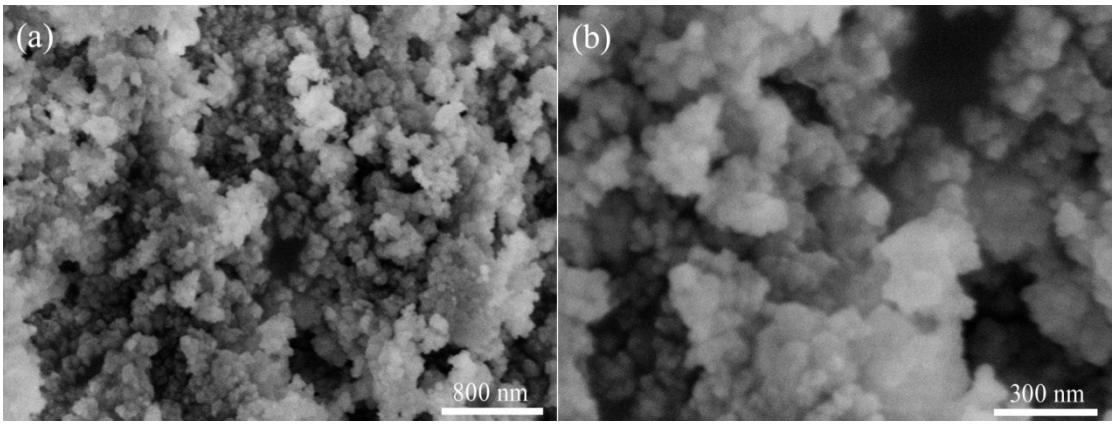

Figure S1. The SEM images of Phy-Co^{2+} at different magnification.

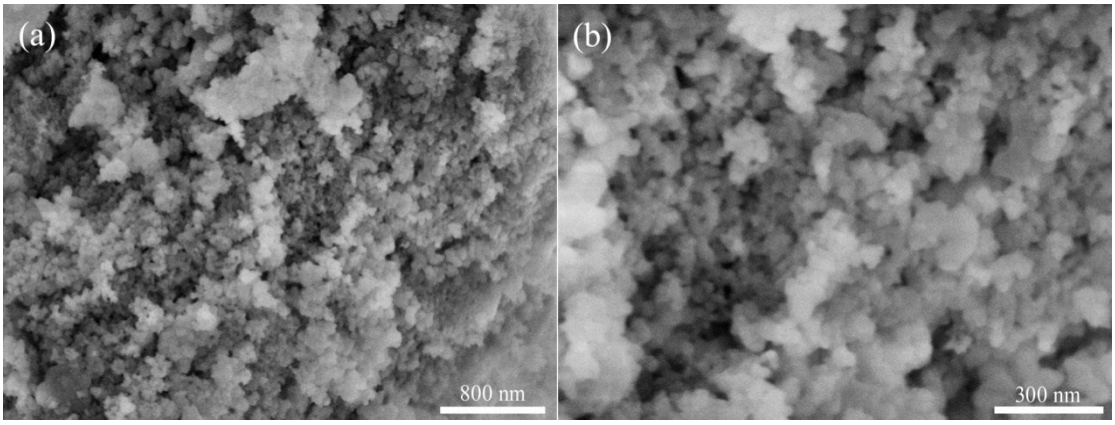

Figure S2. The SEM images of P-Phy-Co^{2+} at different magnification.

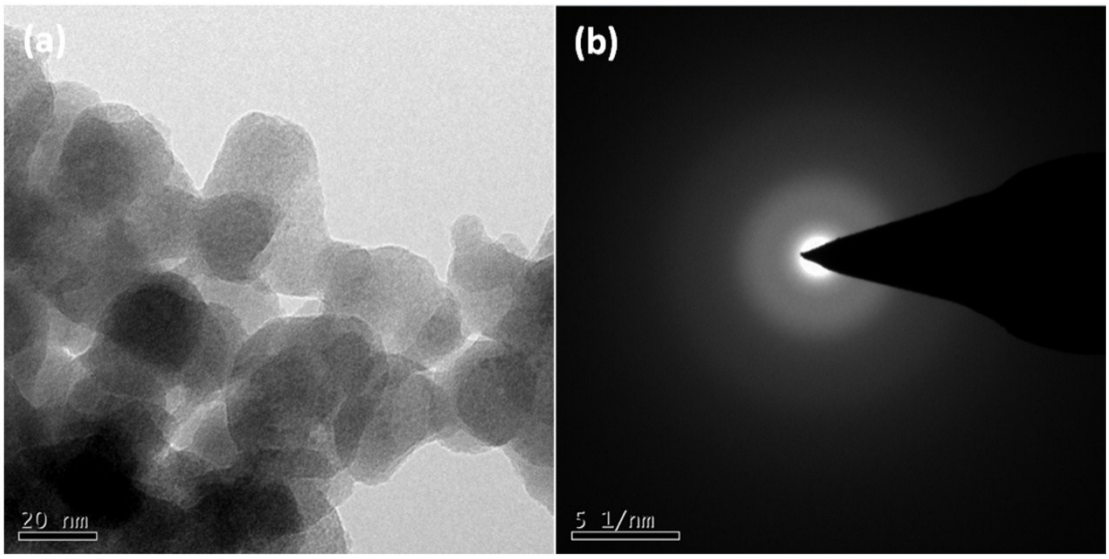

Figure S3. (a) The TEM image of Phy-Co^{2+} and the corresponding SAED pattern of the Phy-Co^{2+}.

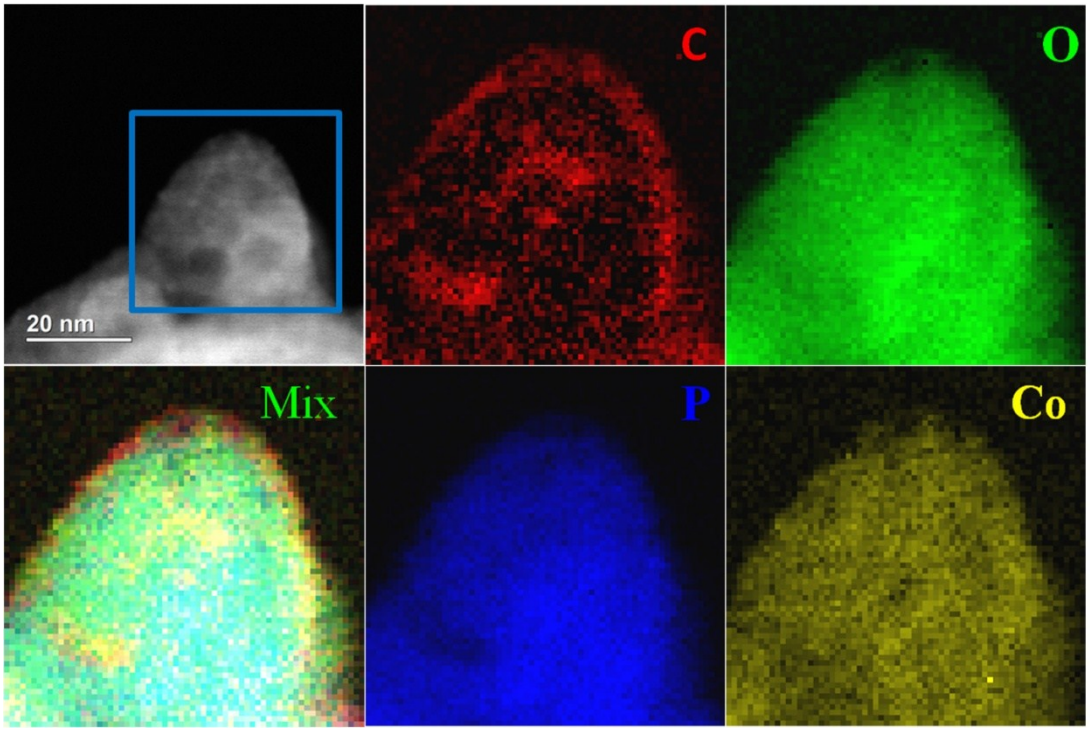

Figure S4. STEM-EELS mapping of Phy-Co^{2+}.

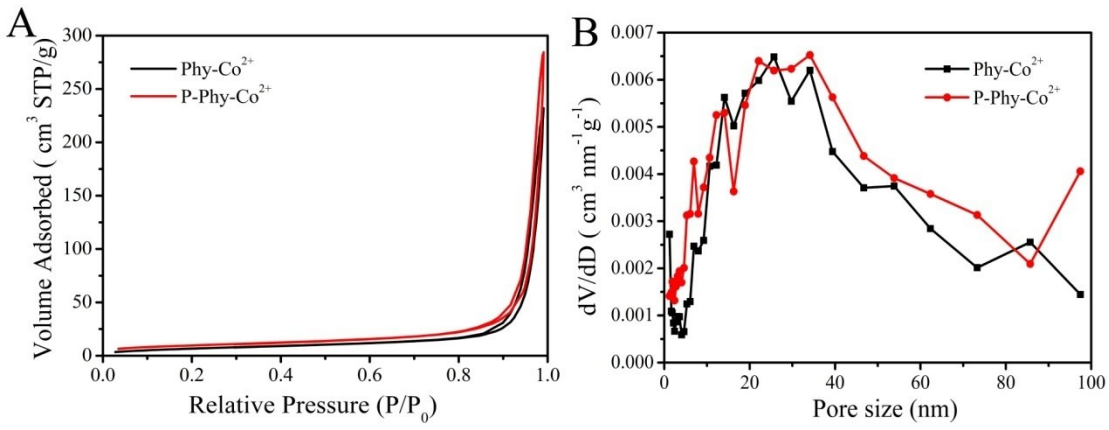

Figure S5. (A) N2 isotherms of Phy-Co^{2+} and P-Phy-Co^{2+}; (B) Pore size distribution of Phy-Co^{2+} and P-Phy-Co^{2+}.

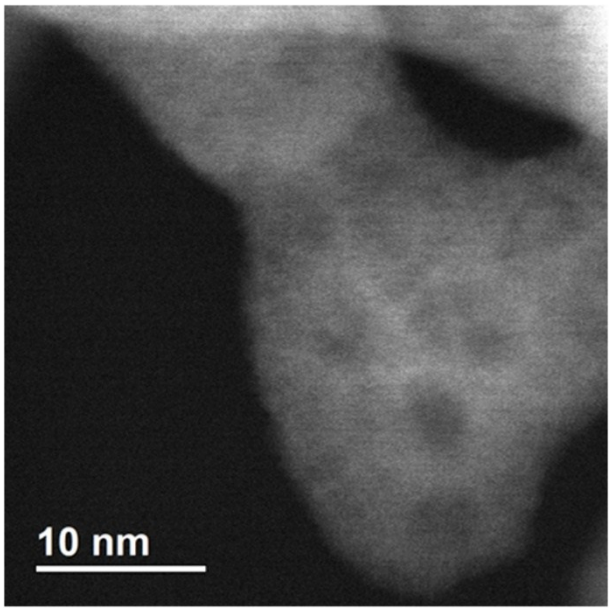

Figure S6. HRTEM image of P-Phy-Co^{2+}.

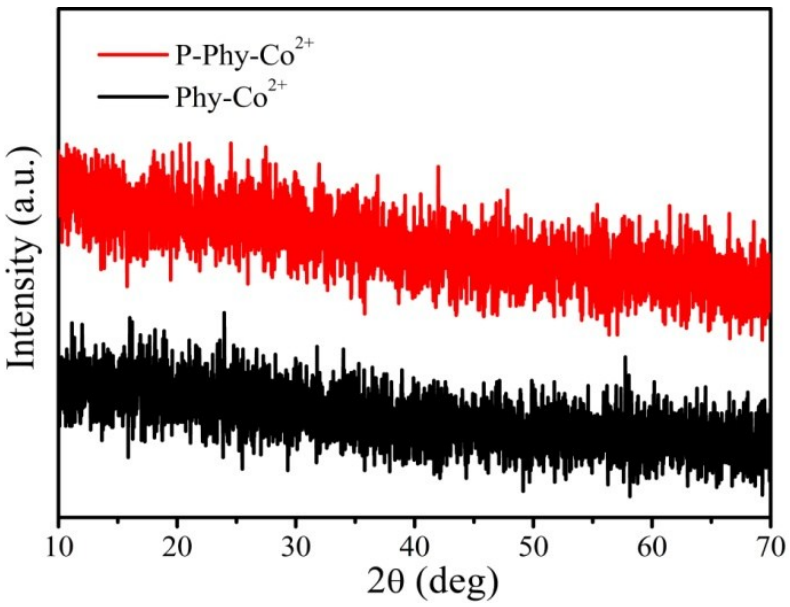

Figure S7. XRD patterns of the Phy-Co^{2+} and P-Phy-Co^{2+}.

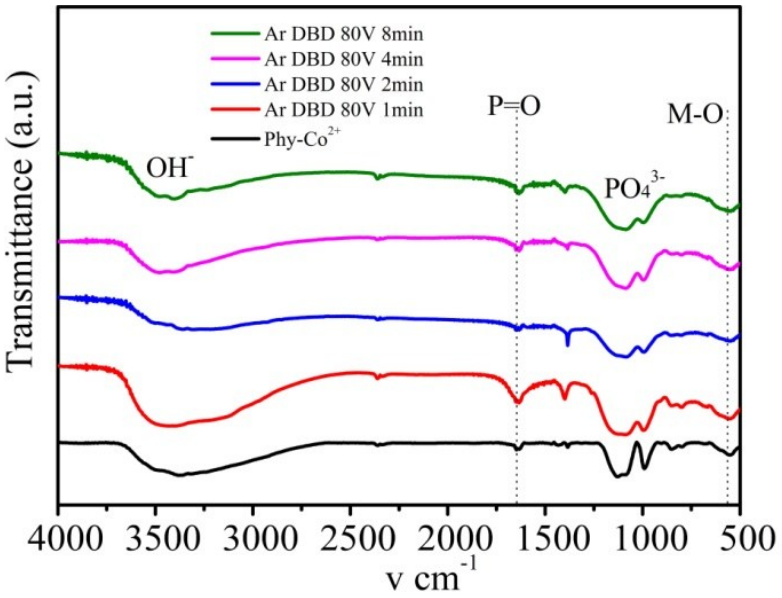

Figure S8. IR spectrum of the Phy-Co^{2+} and P-Phy-Co^{2+}.

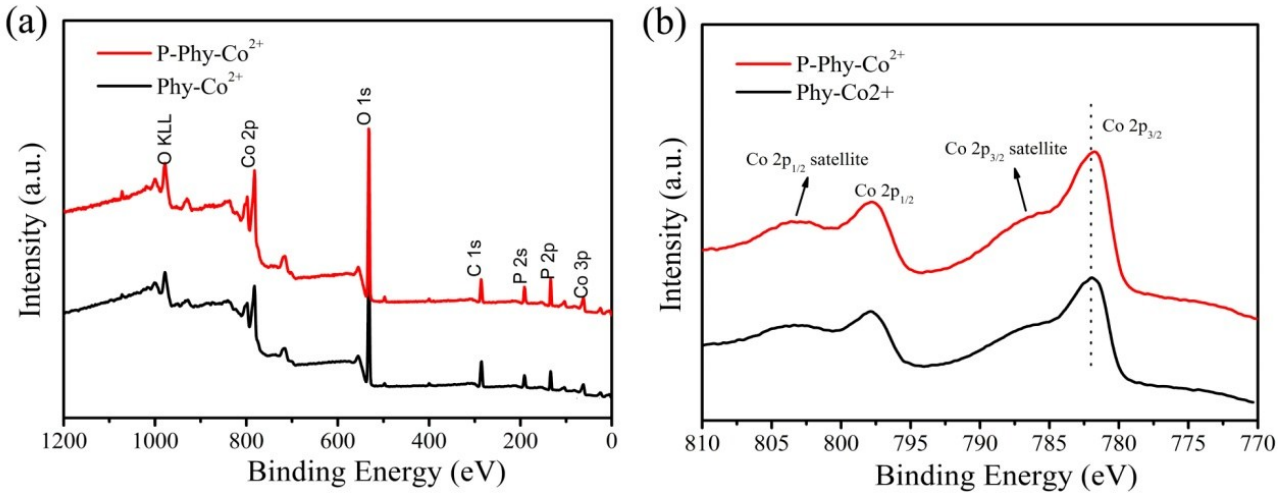

Figure S9. (a) The survey XPS spectra of Phy-Co^{2+} and P-Phy-Co^{2+} and (b) the high-resolution spectra of Co 2p of Phy-Co^{2+} and P-Phy-Co^{2+}.

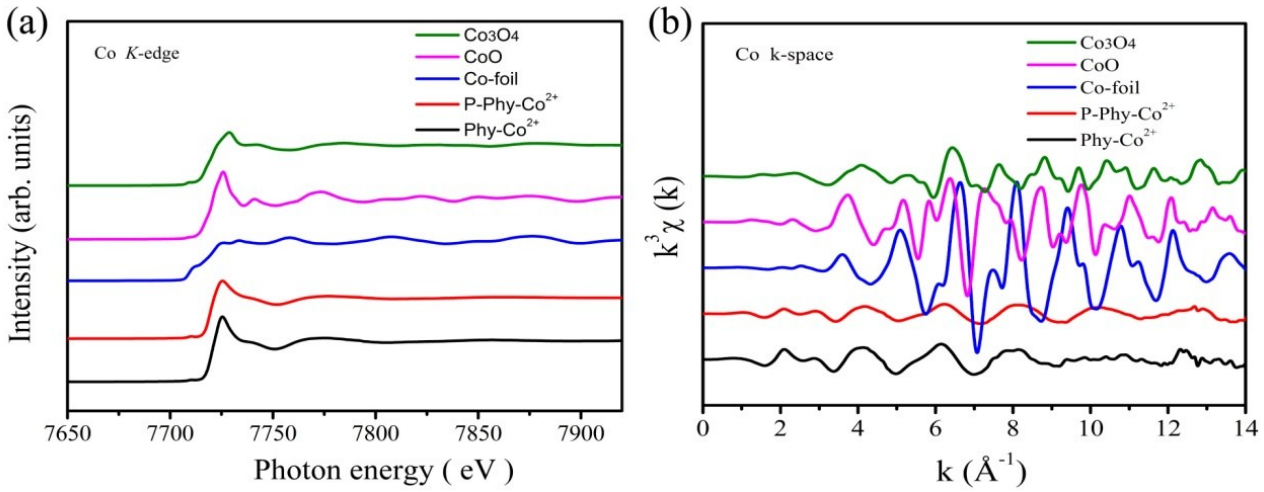

Figure S10. (a) Co K-edge XANES spectra (b) Co K-edge extended XANES oscillation functions $k^3\chi(k)$ of Phy-Co^{2+} and P-Phy-Co^{2+}, and standard Co metal, CoO, and Co_3O_4.

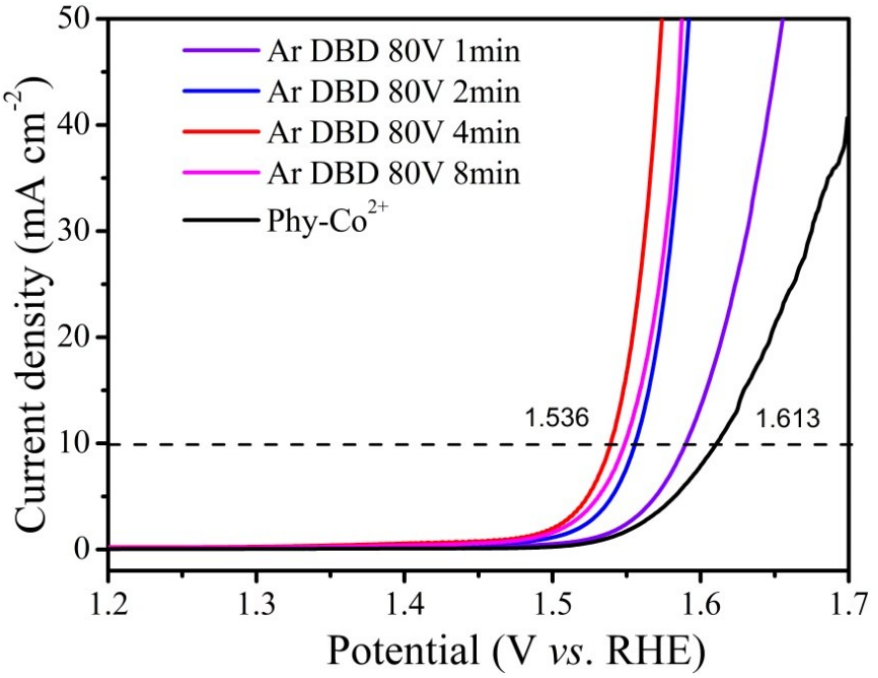

Figure S11. LSV polarization curves Phy-Co^{2+} electrocatalysts by Ar DBD plasma with different time.

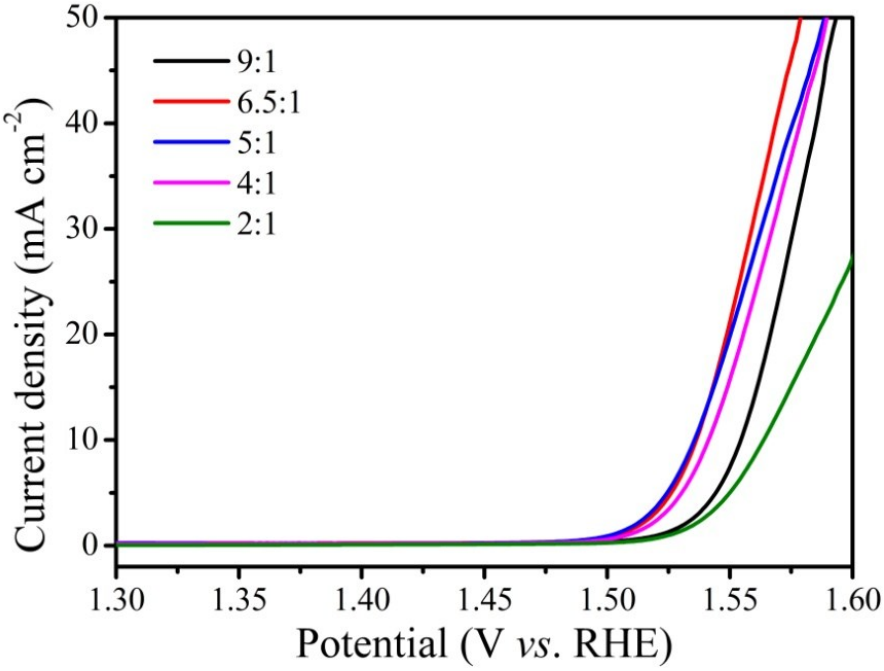

Figure S12. Polarization curves of Phy-Co^{2+}/Fe^{3+} on GCE with different mole ratio with the same loading.

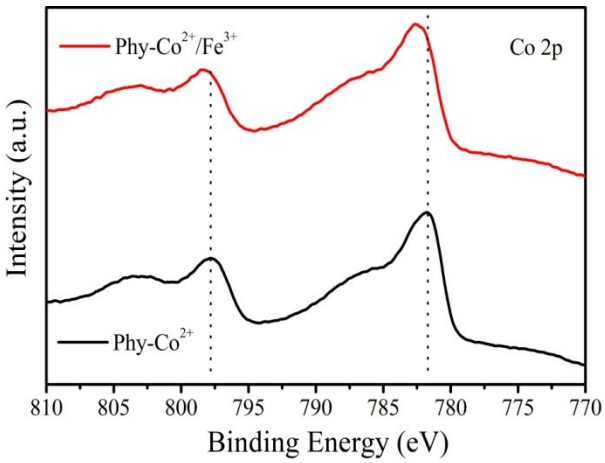

Figure S13. The high-resolution spectra of Co 2p of Phy-Co^{2+} and Phy-Co^{2+}/Fe^{3+}.

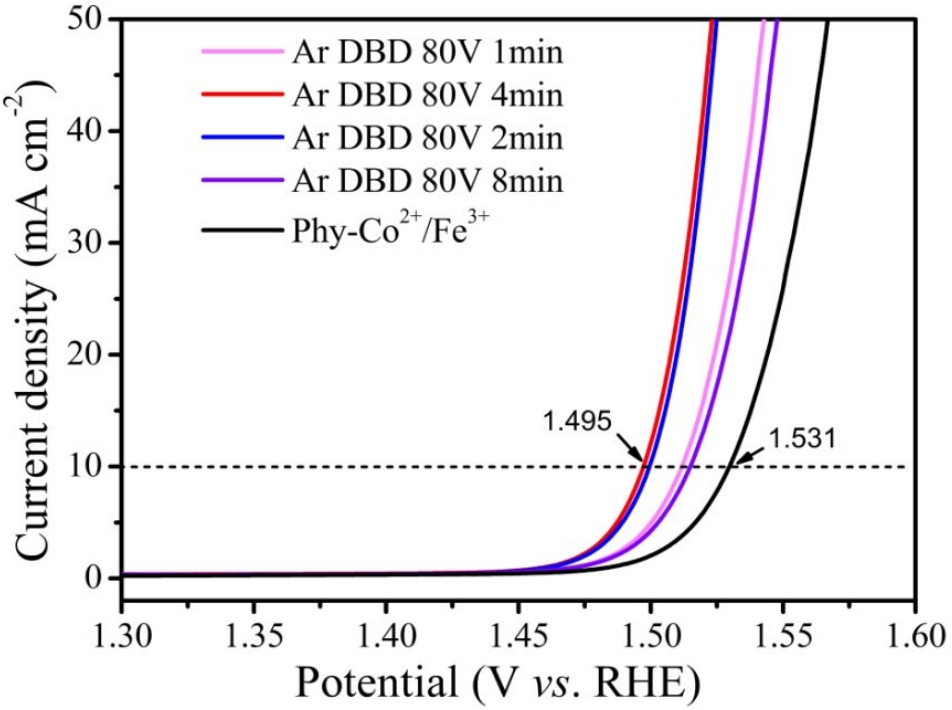

Figure S14. LSV polarization curves Phy-Co^{2+}/Fe^{3+} electrocatalysts by Ar DBD plasma with different time.

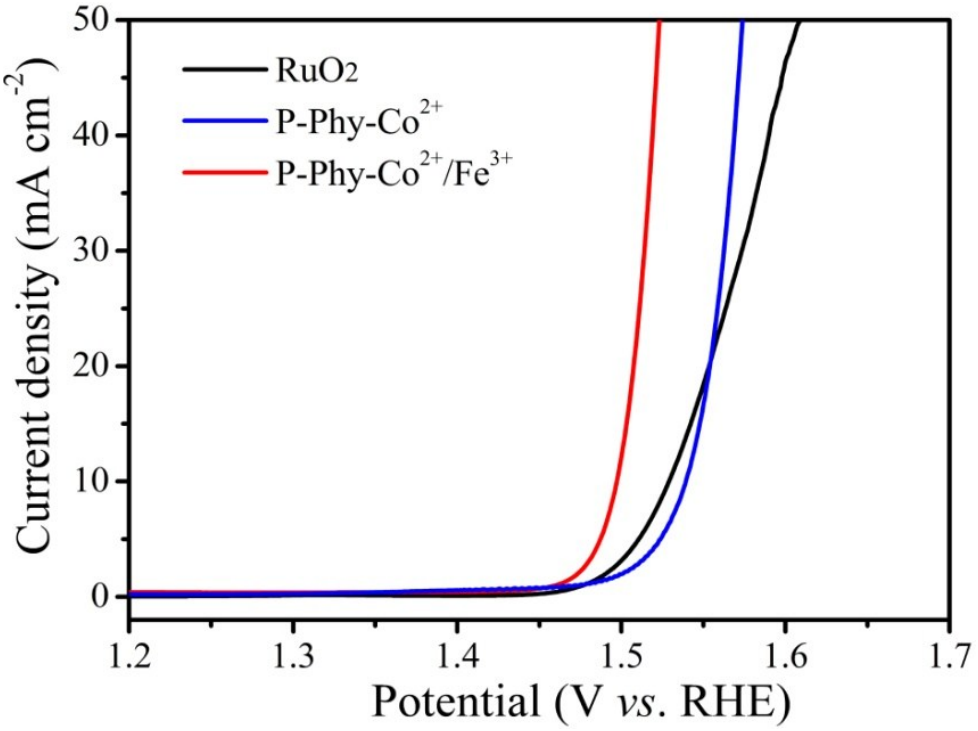

Figure S15. LSV polarization curves of P-Phy-Co^{2+}/Fe^{3+} and P-Phy-Co^{2+} comparison with that of RuO_2.

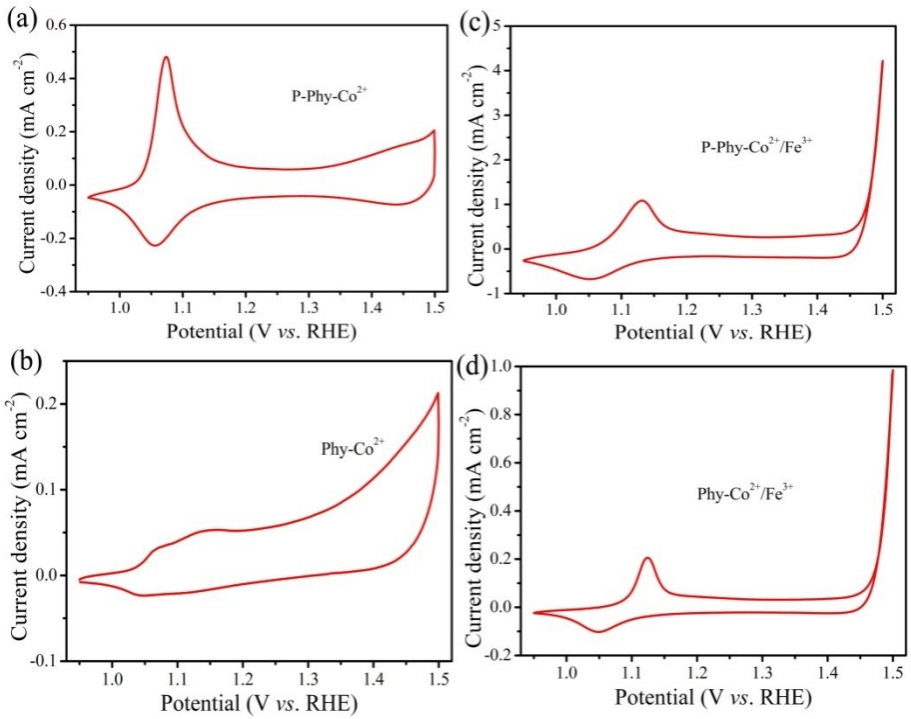

Figure S16. The CVs of (a) Phy-Co^{2+}, (b) P-Phy-Co^{2+}, (c) Phy-Co^{2+}/Fe^{3+} and (d) P- Phy-Co^{2+}/Fe^{3+} electrocatalyst at scan rates of 2 mV s^{-1}.

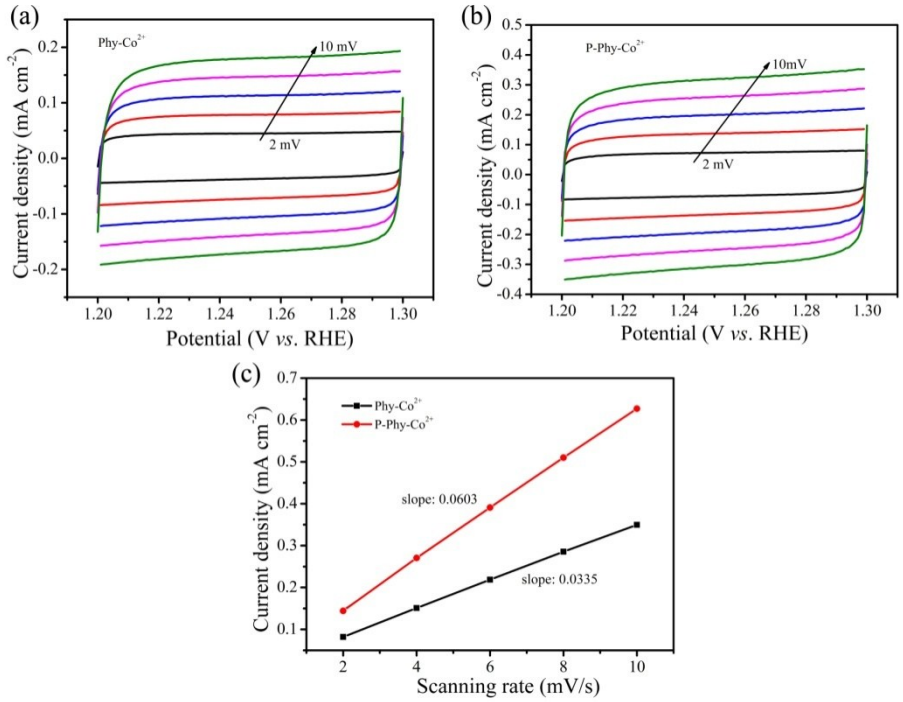

Figure S17. Cyclic voltammetry curves of (a) Phy-Co^{2+}, (b) P-Phy-Co^{2+}, (c) charging current density differences plotted against scanning rates. The linear slope, equivalent to twice the double-layer capacitance, C_{dl}, was used to represent the ECSA.

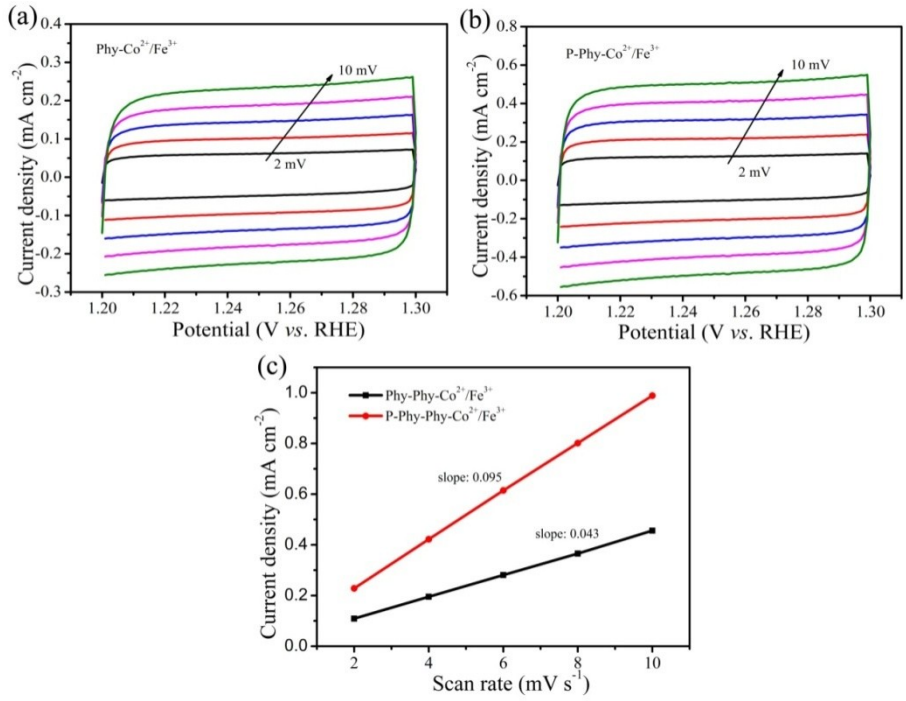

Figure S18. Cyclic voltammetry curves of (a) Phy-Co^{2+}/Fe^{3+}, (b) P-Phy- Co^{2+}/Fe^{3+}, (c) charging current density differences plotted against scanning rates. The linear slope, equivalent to twice the double-layer capacitance, C_{dl}, was used to represent the ECSA.

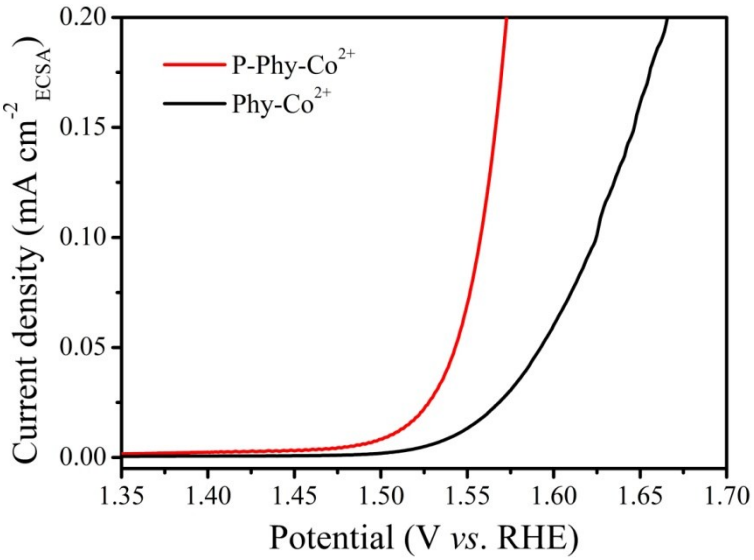

Figure S19. The current was normalized by the ECSA values.

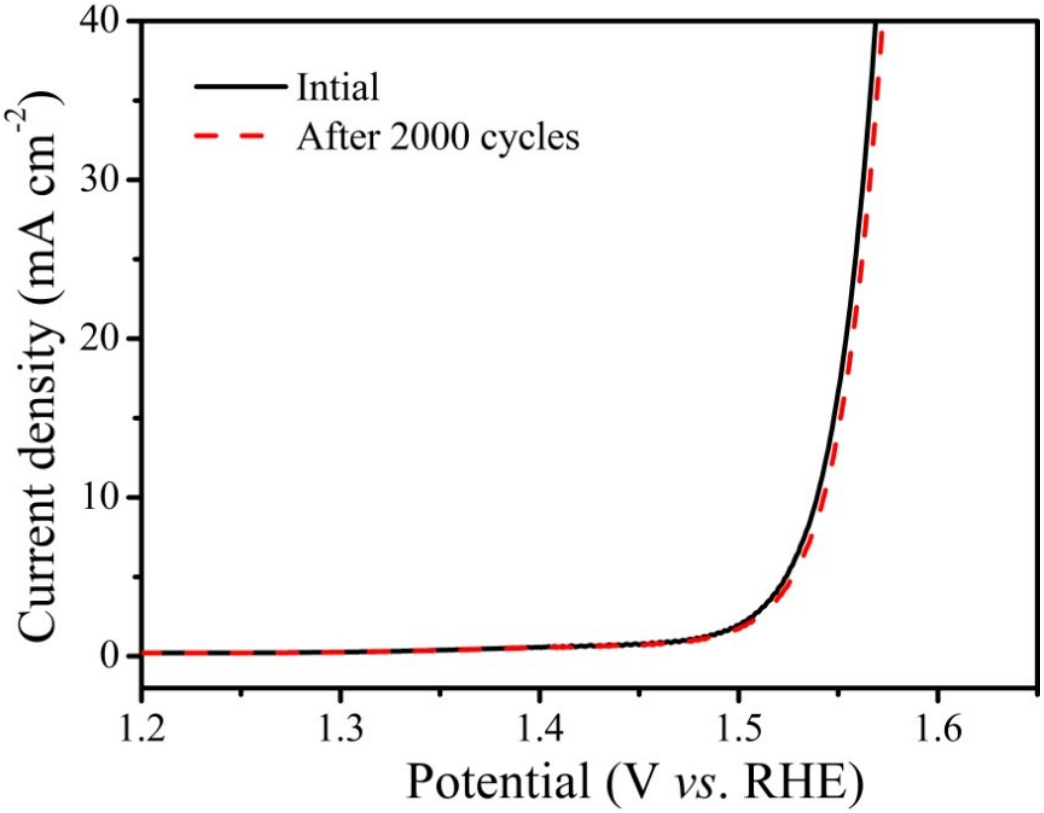

Figure S20. The stability testing of P-Phy-Co^{2+}.

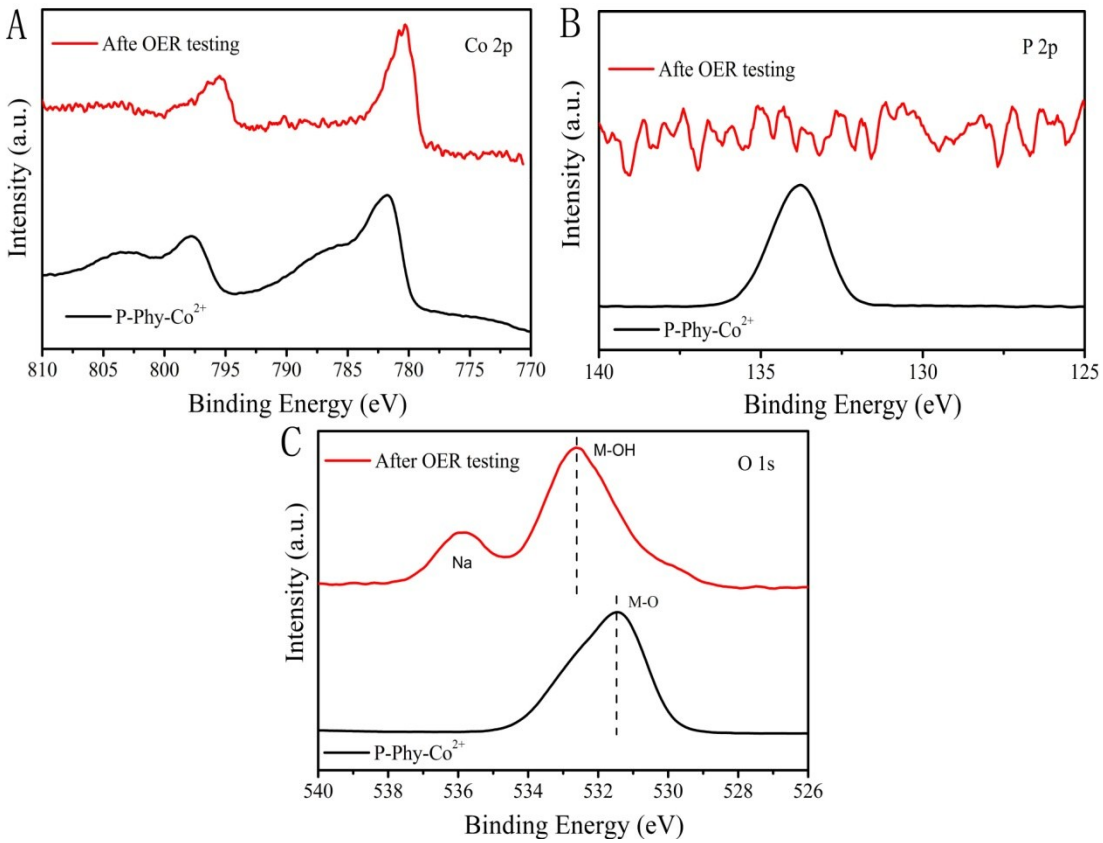

Figure S21. XPS for the P-Phy-Co^{2+} before/after stability test in 1.0 M KOH

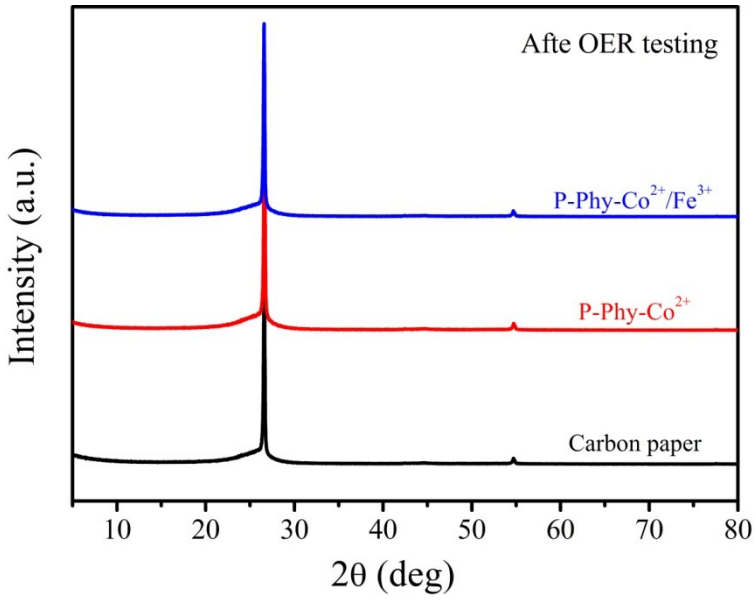

Figure S22. XRD for the P-Phy-Co^{2+} before/after stability test in 1.0 M KOH

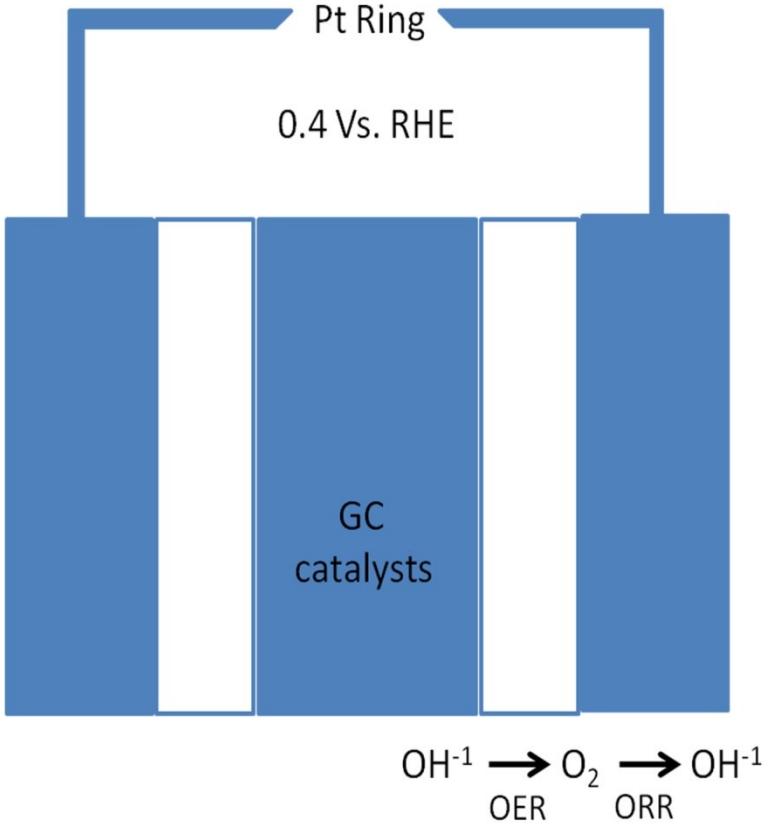

Figure S23. The Faraday efficiency testing mechanism scheme of the RRDE, the blue columns on the sides are Pt ring electrodes. The Pt ring electrode and glassy-carbon electrode are separated by a non-conductive PTFE barrier (white columns). When a constant current (300 μA) is applied to the disk electrode for O_2 generation at 20 s, a ring current of 57.9 μA caused by O_2 reduction is detected immediately.

The Faradaic efficiency (ε) was determined by collecting the ring current when fixing the disk current at 200 μA and ring potential at 0.4 V versus RHE in N_2-saturated 1 m KOH solution

$$\epsilon = \frac{Ir}{Id * N}$$

where I_d is the disk current, I_r is the ring current, and N is the current collection efficiency (0.20 in this study) which was determined by IrO_2 catalyst thin film electrode.

Table S1. Comparison of the OER activity for several recently reported Co-based and CoFe-based highly active noble metal-free catalysts supported on glassy carbon electrode. (η: overpotential at the current density of 10 mA cm^{-2})

Electrocatalysts	*η (mV)*	***Tafel slope (mV dec-1)***	*Electrolyte*	***Reference***
P-Phy-Co^{2+}	*306*	*56.20*	*1 M KOH*	*This work*
Co_3O_4/N-rmGO	*310*	*67*	*1 M KOH*	*Nat. Mater. 2011, 10, 78*
Co_3S_4 nanosheet	*355*	*40*	*0.1 M KOH*	*Angew. Chem. Int.Ed. 2015, 127, 11383.*
Au@Co3O4	*378*	*60*	*1 M KOH*	*Adv. Mater. 2014, 26, 3950.*
CoSe2/N-doped graphene	*366*	*40*	*0.1 M KOH*	*ACS Nano 2014, 8, 3970.*
Ag-$CoSe_2$	*320*	*56*	*1 M KOH*	*Angew. Chem. Int. Ed. 2017, 56,328 –332*
$CoSe_2$	*320*	*44*	*0.1 M KOH*	*J. Am. Chem. Soc. 2014, 136, 15670-15675.*
P-Phy-Co^{2+}/Fe^{3+}	*265*	*36.51*	*1 M KOH*	*This work*
Ni-Co oxides layers	*325*	*39*	*1 M NaOH*	*ACS Nano 2014, 8, 9518.*
Mn-Co oxyphosphide	*320*	*52*	*1 M KOH*	*Angew.Chem. Int. Ed. 2017, 56, 2386 –2389*
Ni-Co Nanowire	*302*	*43.6*	*1 M KOH*	*Adv. Energy Mater. 2017, 7, 1601492*
$FeCoO_X$	*308*	*36.8*	*0.1 M KOH*	*Adv. Mater. 2017, 29, 1606793*
$CoFe_2O_4$/PANI-MWCNTs)	*314*	*30.69*	*1 M KOH*	*J. Mater. Chem. A, 2016, 4, 4472–4478*
RuO_2	*387*	*90*	*0.1 M KOH*	*J. Am. Chem. Soc. 2014, 136, 7077.*
IrOx	*370*	*49*	*1 M KOH*	*J. Am. Chem. Soc.*

				2012, 134, 17253.